35th Annual International Conference of the IEEE EMBS
Osaka, Japan, 3 - 7 July, 2013

Ultrasound Contrast Image Segmentation Using a Modified Level Set Method

Ming Qian, Lili Niu, Yang Xiao, Congzhi Wang, Weibao Qiu, and Hairong Zheng *

Abstract—**Manual segmentation of ultrasound contrast images is time-consuming and inevitable to variability, and computer-based segmentation algorithms often require user interaction. This paper proposes a novel level set model for fully automated segmentation of vascular ultrasound contrast images. The initial contour of arterial boundaries is acquired based on an automatic procedure. The level set model moves the initial contour towards the boundaries of arterial inner wall based on minimization of the energy function. The traditional energy function is improved by introducing an edge detector based on image gradient and the standard difference image. Both spatial and temporal information of the image are considered, and the robustness and accuracy of the level set model is enhanced. Ultrasonic contrast images of living mouse are acquitted with high frequency ultrasound system. Images of carotid arteries are processed with our method. The segmentation results using the proposed method are evaluated against two observers' hand-outlined boundaries, showing that computer-generated boundaries agree well with the observers' hand-outlined boundaries as much as the different observers agree with each other.**

I. Introduction

Hemodynamic parameters and arterial wall biomechanical properties are two important determinants of various cardiovascular diseases. Local hemodynamic factors participate in the physiopathology of atherogenesis, accounting for the focal nature of the atherogenic process [1], [2]. In a correlation-based image processing of two consecutive ultrasound contrast images of arterial flow, an interrogation window that contains the regions of blood flow and arterial wall respectively can be used to calculate hemodynamic parameters[3]–[5], and arterial elasticity [6]–[9]. The accurate delineation of arterial inner wall in ultrasound contrast images can obtain the exact interrogation window for the image processing.

Considerable efforts have been made to develop effective ultrasound image segmentation methods for computer-aided diagnosis. A sophisticated threshold method was proposed to segment the ultrasound image that the object to be detected is homogeneous [10], but it is not applicable for the inhomogeneous ultrasound contrast images. A dynamic programming method was used to search for global minimum of cost function which takes intensity and gradient into account [11], [12]. However, it is not able to capture deep concavities and sharp salience. A snake method was developed to segment the intima-media layer of far wall of common carotid artery (CCA) [13]. The problem is that snake-based methods may converge to wrong location if the initial contour is placed far away from the region of interest. Region growing based on window frame difference was proposed to detect the arterial inner wall in ultrasound particle image of both CCA and carotid bifurcation artery (CBA) [14]. Post processing, such as edge-linking, holes filling, is necessary to obtain the final boundaries. Level set active contour is a popular method in medical image segmentation due to several desirable advantages. First, it allows flexible topological changes of the evolution curve. Second, it produces continuous and smooth results. Third, it's easily formulated under an energy optimization framework.

This paper presents a modified level set method which considers both the spatial and temporal information of the raw image for fully automated segmentation of vascular ultrasound contrast images.

II. Materials and Methods

A. Acquisition of ultrasound contrast image sequence

The carotid arteries of 12 healthy mice were scanned in B-mode. All procedures in the animal studies adhered to our institution's Animal Care and Use Committee guidelines. The age of the subjects was ranging from 8 to 12 weeks. Each mouse was anesthetized with isoflurane gas and laid on a platform in the supine position with legs taped to electrocardiographic electrodes for heart rate monitoring (380 beats/min). Body temperature was maintained around 37 °C. The neck hair of each mouse was gently removed. After the mouse and the transducer were settled, UCAs were injected via caudal vein. The bubble concentration was about 10^7 bubbles/ml and the injection capacity adjusted according to the weight of the mouse. B-mode images of the mouse carotid artery were acquired by a Vevo2100 device (VisualSonics, Toronto, Canada) with a 30MHz MS-400 probe. The focal position was set at a depth of 8 mm to 11 mm.. All images were acquired with a frame rate up to 712 fps. For each mouse, frames were recorded so as to cover more than 2 cardiac cycles. Fig. 1(a) and 1(b) show the representative ultrasound contrast images of mouse carotid arteries.

* The work was supported by National Basic Research Program 973 (Grant Nos. 2010CB732605, 2010CB534914) from Ministry of Science and Technology, China, National Science Foundation Grants (Grant No. 11272329, 11002152, 81027006, 61020106008, and 61002001), National Key Technology R&D Program(Grant No. 2012BAI13B01), Guangdong Basic Research Grant, Shenzhen International Collaboration Grant, Shenzhen Basic Research Grant.

First Author Ming Qian and corresponding author Hairong Zheng, and co-authors Lili Niu, Yang Xiao, Congzhi Wang, Weibao Qiu are with Shenzhen Institutes of Advanced Technology, Chinese Academy of Sciences, Shenzhen, China 518055. (e-mail: ming.qian@siat.ac.cn; hr.zheng@siat.ac.cn).

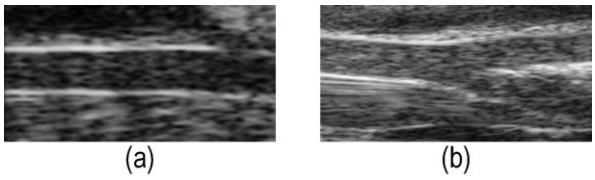

Fig. 1. Ultrasound contrast images of the mouse carotid arteries: (a) Common carotid artery, (b) Carotid bifurcation artery.

B. Contour initialization

Arterial blood flow and microbubbles therein move much faster than arterial wall and surrounding tissue. For consecutive ultrasonic contrast images, the intensity difference in the lumen region is much bigger than in the regions of arterial wall and tissue. The standard difference of several consecutive images can enhance the lumen region and suppress the regions of arterial wall and surrounding tissue. The standard difference matrix of a sequence of 2k+1 consecutive frames was defined as

$$D(x,y)=\left[\frac{1}{2k}\sum_{t=-k}^{k}\left(I_t(x,y)-\bar{I}(x,y)\right)^2\right]^{\frac{1}{2}} \tag{1}$$

$I_0(x,y)$ raw image, $\bar{I}(x,y)$ mean value of the 2k+1 consecutive images. Seven consecutive images were used and the standard difference images were shown in Fig. 2.

An automatic method based on morphological filtering and thresholding is applied to the standard difference image to provide initial contour. The initialization procedure for both mouse CCA and CBA is as follows:

1) Load the standard difference image (see Fig.2).
2) Perform gray scale opening and closing on the standard difference image to eliminate sharp peaks and small islands in image [15]. They are presented as

$$G(x,y)=\left(D(x,y)\circ SE\right)\bullet SE \tag{2}$$

where $D(x,y)$ is the standard difference image, SE is the structure element, $G(x,y)$ is the image obtained after opening and closing process. SE was chosen as 9×9 for this step.

3) Convert the image $G(x,y)$ to binary by thresholding [16]. Apply binary opening and closing to fill gaps and eliminate peaks to make the initial contour smooth. By superimposing the contours on the original images, the initial contour of mouse CCA and CBA were obtained.

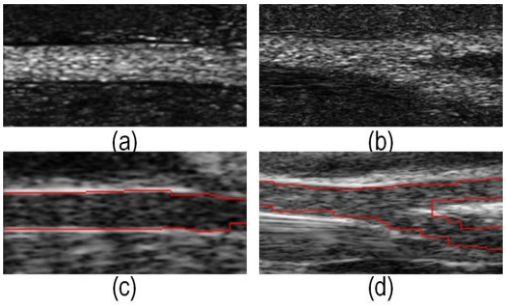

Fig. 2. The standard difference images of the ultrasound contrast images of mouse carotid arteries based on 7 consecutive images: (a)CCA, (b) CBA . The initial contour overlapped on the raw image. (c)CCA, (d) CBA.

C. The modified level set model

As a self-adapting model, level set method moves the initial contour towards the boundaries of object based on minimization of an energy function. Generally, iterative algorithm is used to solve the problem. The energy function is defined as follows [17].

$$\begin{aligned}F(c_1,c_2,C)&=\mu\,\mathrm{Length}(C)+\lambda_1\int_{\mathrm{inside}(C)}\left|u_0(x,y)-c_1\right|dxdy\\&+\lambda_2\int_{\mathrm{outside}(C)}\left|u_0(x,y)-c_2\right|dxdy\end{aligned} \tag{3}$$

where $u_0(x,y)$ is the image to be segmented, C is the evolving curve, c_1 and c_2 represent average intensity inside and outside C respectively, μ is a smoothing coefficient and should be positive, λ_1 and λ_2 weight the function.

The evolving curve C in Ω is defined as the boundary of an open subset ω ($\omega\subset\Omega$) which is the region inside C. The region outside C is denoted as $\Omega\setminus\varpi$. The evolving curve C can be represented as $C=\{(x,y)\mid\phi(x,y)=0\}$ [18], where $\phi(x,y)$ is a Lipschitz-continuous function known as the level set function that satisfies

$$\begin{cases}\phi(x,y)>0;\forall(x,y)\in\omega\\ \phi(x,y)<0;\forall(x,y)\in\Omega\setminus\varpi\\ \phi(x,y)=0;\forall(x,y)\in C=\partial\omega\end{cases} \tag{4}$$

Then, the energy function is formulated as

$$\begin{aligned}F(c_1,c_2,\phi)&=\mu\int_\Omega\delta(\phi)\left|\nabla\phi\right|dxdy\\&+\lambda_1\int_\Omega\left|D(x,y)-c_1\right|H(\phi)\,dxdy\\&+\lambda_2\int_\Omega\left|D(x,y)-c_2\right|\left(1-H(\phi)\right)dxdy\end{aligned} \tag{5}$$

H is Heaviside function. The function δ, termed as Dirac function, is derivative of H. $D(x,y)$ the standard difference images.

An edge detector which depends on the gradient of the image was introduced. Generally, g is defined as below [22]

$$g=\frac{1}{1+\left|\nabla G_\sigma * I\right|^2}, \tag{6}$$

where G_σ is Gaussian kernel with standard deviation σ, and I is the raw image.

However, the edge detector g in equation (6) is not suitable for ultrasound contrast images. The reasons are: 1) existence of bright speckles in the ultrasound contrast image makes the intensity gradient at the arterial wall much smaller, 2) Gaussian smoothing is isotropic diffusion which will smooth edge, and the curve may pass through the boundary and stop in the wrong position. Thus, an edge detector should be constructed considering the inherent properties of ultrasound contrast images.

In this study, a new edge detector is constructed by following two steps. First, the raw ultrasound contrast image is subjected to a median filter and normalization process to make

the lumen homogenous and boundaries enhanced. The ultrasound contrast images are degraded by speckle noises and the existence of contrast agents makes the lumen region inhomogeneous and the arterial boundaries ambiguous. An adaptive weighted median filter is used to reduce the intensity variance in the lumen [19]. The filter image can be obtained as:

$$J(X) = \underset{(X)\in[m,n]}{median}\left[\sum_{t=-k}^{k} I_t(X)\right] \quad (7)$$

where $(X)=(x,y)$, $I_0(X)$ is the raw image and $I_{-k}(X)$ to $I_k(X)$ are the $(2k+1)$ frames before and after the raw image respectively, $\underset{(X)\in[m,n]}{median}[\cdot]$ denotes a median filter operator with a window size of $m \times n$.

An image normalization method is followed [20]. Linear scaling of the image was performed by contrast stretch, histogram normalization and equalization. It can reduce the variability introduced by different equipments, operators, and gain settings, and to facilitate ultrasound tissue comparability [21].

The second step is to apply the gradient vector flow algorithm to the filtered and normalized image $J(X)$ to acquire the vector field and construct the edge detector. The gradient vector flow (GVF) is an edge preserving process that has the ability to move the contour into boundary concavities [22]. GVF is defined as the vector field $V(X)=(u,v)$ that minimizes the energy function

$$\varepsilon = \iint \alpha \left|\nabla V(X)\right|^2 + \left|\nabla J(X)\right|^2 \left|V(X)-\nabla J(X)\right|^2 dX \quad (8)$$

where $J(X)$ is the filtered and normalized image. The parameter α governs the tradeoff between the first term and the second term of the integrand. The variational formulation of GVF makes the vector field has the property that it is nearly equal to the gradient of image at the boundary. The $V(X)$ can be found by solving a pair of Euler equations iteratively [23]. The edge detector, g, in this novel level set model is constructed as,

$$g = \frac{1}{1+\left|V(X)\right|^2} \quad (9)$$

The energy function is finally defined as:

$$\begin{aligned} F(c_1,c_2,\phi) = {} & \mu\int_\Omega g\,\delta(\phi)\left|\nabla\phi\right|dxdy \\ & + \lambda_1\int_\Omega \left|D(x,y)-c_1\right|H(\phi)\,dxdy \\ & + \lambda_2\int_\Omega \left|D(x,y)-c_2\right|\left(1-H(\phi)\right)dxdy \end{aligned} \quad (10)$$

The level set model investigates the evolution of ϕ under the level set partial differential equation [24]:

$$\frac{\partial\phi}{\partial t} = \delta(\phi)\left[\mu\, div\left(g\frac{\nabla\phi}{\left|\nabla\phi\right|}\right) - \lambda_1\left(D-c_1\right)^2 + \lambda_2\left(D-c_2\right)^2\right] \quad (11)$$

where parameter λ_1, λ_2 and μ are positive, besides, μ is smooth coefficient which controls the smoothness of the evolving contour.

III. RESULTS

A series of 20 CCA and 20 CBA ultrasound contrast images of mice were used for validation. The proposed level set model was validated against manual delineations by two experts who know ultrasound contrast images very well. The average of the two manual delineations was considered as ground truth. A statistical and quantitative approach was used for performance evaluation.

Ultrasound contrast images of mouse CCA and CBA are segmented using manual delineation, and the proposed level set model, and the results are presented in Fig. 3. The average of manual delineations of two expert radiologists was set to be ground truth, as shown in Fig. 3(a) and 3(b). The performances of the proposed level set model were demonstrated in Fig. 3(c) and 3(d). It is found that both CCA and CBA segmentation results of level set model are in good agreement to the ground truth.

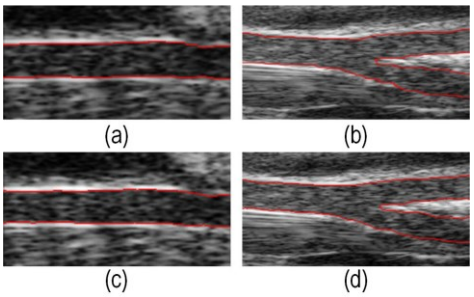

Fig. 3. Segmentation results of ultrasound contrast images of mouse carotid arteries using the manual delineation, and the proposed level set model.

In this paper, an overlap measure termed similar index was used for comparing the relative overlap value of two binary segmentation results. The similar index between automatic segmentation area and the ground truth is defined as follows:

$$S = \frac{A \,\mathrm{I}\, T}{A \,\mathrm{U}\, T} \quad (12)$$

where A is the segmentation area, T is the ground truth, I is intersection, U is union. The more match two segmentations are, the closer S is to 1. S_{LS} is the similar index between the level set model and the ground truth. S_M is the similar index between two experts' manual delineations. The inter-observer variability (S_M) was calculated as 0.91 ± 0.02 on mouse CCA images, and 0.89 ± 0.06 on mouse CBA images. S_{LS} is 0.91 ± 0.01 on mouse CCA, and 0.88 ± 0.04 on mouse CBA. The time needed for segmenting one mouse CCA and CBA image is 6 and 11 seconds using the level set method.

IV. CONCLUSION

This paper proposes a level set approach for fully automated segmentation of vascular ultrasound contrast images. Our approach adopts an automatic initial contour acquisition procedure and a modified level set model that integrates both temporal and spatial image information. Ultrasound contrast images of mouse CCA and CBA were

acquired with high frame rate for performance evaluation of the approach. The segmentation results of the level set approach are evaluated against two observers' hand-outlined boundaries, showing that computer-generated boundaries agree with the observers' hand-outlined boundaries as much as the different observers agree with each other. In the future, we plan to test this level set approach in ultrasound contrast images of arteries with complex geometries like arteries with plaques or thrombosis.

REFERENCES

[1] Y. N. Jiang, K. Kohara, and K. Hiwada, "Association between risk factors for atherosclerosis and mechanical forces in carotid artery," *Stroke*, vol. 31, pp. 2319-2324, Oct. 2000.

[2] C. Cheng, D. Tempel, R. van Haperen, A. van der Baan, F. Grosveld, M. Daemen, R. Krams, R. D. Crom, "Atherosclerotic lesion size and vulnerability are determined by patterns of fluid shear stress," *Circulation*, vol. 113, pp.2744-2753, Jun. 2006.

[3] H. Zheng, L. Liu, L. Williams, J. R. Hertzberg, C. Lanning, and R. Shandas, "Real time multicomponent echo particle image velocimetry technique for opaque flow imaging," *Appl. Phys. Lett.*, vol. 88, 261915, Jun. 2006

[4] M. Qian, L.L. Niu, L. Yan, B. Jiang, Q.F. Jin, C.X. Jiang, and H.R. Zheng, "Measurement of flow velocity fields in small vessel-mimic phantoms and vessels of small animals using micro ultrasonic particle image velocimetry (microEPIV)," *Phys. Med. Biol.*, vol. 55, pp. 6069-6088, Oct. 2010.

[5] L.L. Niu, M. Qian, L. Yan, W.T. Yu, B. Jiang, Q.F. Jin, Y.P. Wang, and H.R. Zheng, "Real-Time Texture Analysis for Identifying Optimum Microbubble Concentration in 2D Ultrasonic Particle Image Velocimetry," *Ultrasound Med. Biol.*, vol. 37, pp. 1280-1291, Aug. 2011.

[6] A.P.G. Hoeks, C.J. Ruissen, P. Hick, R.S. Reneman, "Transcutaneous detection of relative changes in artery diameter," *Ultrasound Med. Biol.,* vol. 11, pp. 51-59, 1985.

[7] S.I. Rabben, S. Bjaerum, V. Sorhus, H. Torp, "Ultrasound-based vessel wall tracking: an auto-correlation technique with RF center frequency estimation," *Ultrasound Med Biol.*, vol. 28, pp.507-517, Apr. 2002.

[8] S. Golemati, A. Sassano, M.J. Lever, A.A. Bharath, S. Dhanjil, A.N. Nicolaides, "Carotid artery wall motion estimated from B-mode ultrasound using region tracking and block matching," *Ultrasound Med. Biol.*, vol. 29, pp.387-399, 2003.

[9] T. Zakaria, Z. Qin, R.L. Maurice, "Optical-flow-based B-mode elastography: application in the hypertensive rat carotid," *IEEE Trans. Med. Imaging*, vol. 29, pp.570-578, Feb. 2010

[10] Y. Zimmer, R. Tepper and S. Akselrod, "A two-dimensional extension of minimum cross entropy thresholding for the segmentation of ultrasound images," *Ultrasound Med. Biol.*, vol. 22, pp. 1183-1190, 1996.

[11] Y. B. Lee, Y. J. Choi, and M. H. Kim, "Boundary detection in carotid ultrasound images using dynamic programming and a directional Haar-like filter," *Comput. Biol. Med.*, vol. 40, pp. 687-697, Aug. 2010.

[12] Q. Liang, I. Wendelhag, J. Wikstrand and T. Gustavsson , "A multiscale dynamic programming procedure for boundary detection in ultrasonic artery images", *IEEE Trans. Med. Imaging*, vol. 19, pp.127-42, Feb. 2000.

[13] C. P. Loizou, C. S. Pattichis, M. Pantziaris, T. Tyllis and A. Nicolaides, "Snakes based segmentation of the common carotid artery intima media", *Med. Biol. Eng. Comput.*, vol.45, pp.35-49, Jan. 2007.

[14] F. Zhang, L.O. Murta, J.S. Chen, A.J. Barker, L. Mazzaro, C. Lanning , R. Shandas, "Evaluation of segmentation algorithms for vessel wall detection in echo particle image velocimetry", *IEEE International Ultrasonics Symposium*. Rome, Italy: Institute of Electrical and Electronics Engineers Inc.. pp. 2476-79, 2009.

[15] B. Jiang, M. Qian, L.L. Niu, R.B. Song, H.C. Zhu, Q.F. Jin, and H.R. Zheng, "Region Growing Based on Window Frame Difference for Segmenting Ultrasound Contrast Images of Arteries", *The 5th International Conference on Bioinformatics and Biomedical Engineering Wuhan China, May 10-12, 2011*.

[16] T. Chan and L. Vese, "Active Contours without Edges," *IEEE Trans. Image Process.*, vol. 10, pp. 266-277, Feb. 2001.

[17] A. C. Rossi, P. J. Brands, A. P. G. Hoeks, "Automatic localization of intimal and adventitial carotid artery layers with noninvasive ultrasound: a novel algorithm providing scan quality control," *Ultrasound Med. Biol.*, vol.36, pp.467-479, Mar. 2010.

[18] F. Molinari, G. Zeng, J.S. Suri, "Intima-Media Thickness: Setting a Standard for a Completely Automated Method of Ultrasound Measurement," *IEEE Trans. Ultrasonics Ferroelectrics and Frequency Control*, vol. 57, pp. 1112-1124, 2010

[19] R. M. Haralick, S. R. Stemberg and X. Zhuang, "Image analysis using mathematical morphology," *IEEE Trans. Pattern Anal. Machine Intell.*, vol.PAMI-9, pp.532-550,1987.

[20] N. Otsu, "A threshold selection method from gray-level histogram", *IEEE Trans. Syst. Man. Cybern.*, vol. 9, pp. 62-66, 1979.

[21] S. Osher and J. A. Sethian, "Fronts Propagating with Curvature-dependent Speed: Algorithms Based on Hamilton–Jacobi Formulation", *J. Comput. Phys.*, vol. 79, pp. 12-49, 1988

[22] C. Li, C. Xu, C. Gui and M. D. Fox, "Level set evolution without re-initialization: A new variational formulation", *Proc. IEEE Conf. Computer Vision and Pattern Recognition*, vol. 1, pp.430-437, 2005.

[23] T. Loupas, W. N. Mcdicken, and P. L. Allan, "An adaptive weighted median filter for speckle suppression in medical ultrasonic images", *IEEE Trans. Circuits Syst.*, vol. 36, pp.129–135, 1989.

[24] C. P. Loizou, C. S. Pattichis, I. Seimenis and M. Pantziaris, "Quantitative analysis of brain white matter lesions in multiple sclerosis subjects," *Proc. 9th Int. Conf. Inform. Techn. Appl. Biomed., ITAB*, pp.1-4, 2009.